

iron sulfides are thought by some to be energy sources for early life forms (25). Nanometer-scale pyrrhotite and possibly greigite were reported in the martian meteorite ALH84001 and were cited as evidence for ancient life on Mars (26). As we found neither pyrrhotite nor pyrite in terrestrial magnetotactic bacteria, their presence in ALH84001 appears to be irrelevant to the question of possible former biogenic activity on Mars. Greigite, which was also mentioned as a possible phase in ALH84001 (26), is the most abundant sulfide in magnetotactic bacteria and could be the best, although not an unambiguous, indicator of past biogenic activity.

Both greigite and mackinawite convert to smythite in hydrothermal ore specimens (27). When heated above 238°C in vacuum, greigite breaks down to pyrrhotite (28); in addition, in many marine sediments mackinawite reacts to greigite and then to pyrite (15, 29). Clearly, greigite can transform into at least three different phases, depending on its thermal and chemical environment. Characterization of sulfide minerals and morphologies, together with reliable knowledge about the thermal history of the specimen, is needed to provide useful information about a bacterial origin of Fe sulfides in extraterrestrial samples.

REFERENCES AND NOTES

1. M. Farina, H. Lins de Barros, D. Motta de Esquivel, J. Danon, *Biol. Cell.* **48**, 85 (1983); F. G. Rodgers *et al.*, *Arch. Microbiol.* **154**, 18 (1990).
2. D. A. Bazylinski, R. B. Frankel, A. J. Garratt-Reed, S. Mann, in *Iron Biominerals*, R. B. Frankel and R. P. Blakemore, Eds. (Plenum, New York, 1990), pp. 239–255.
3. B. R. Heywood, S. Mann, R. B. Frankel, *Mater. Res. Soc. Symp. Proc.* **218**, 93 (1991).
4. S. Mann, N. H. C. Sparks, R. B. Frankel, D. A. Bazylinski, H. W. Jannasch, *Nature* **343**, 258 (1990).
5. M. Farina, D. M. S. Esquivel, H. G. P. Lins de Barros, *ibid.*, p. 256.
6. D. A. Bazylinski and B. M. Moskowitz, *Rev. Mineral.* **35**, 181 (1997).
7. After deposition on the TEM grids, the bacterial cells were dried in air and were kept in a grid box in air before and between TEM studies. We used a JEOL 2000FX TEM operated at a 200-kV accelerating voltage and equipped with a double-tilt ($\pm 30^\circ$, $\pm 45^\circ$) goniometer stage. TEM images were used to observe particle morphologies and structural defects. Compositions were determined by energy-dispersive x-ray spectrometry with an attached ultrathin-window KEVEX detector. Experimental *k*-factors for thin-film analysis were determined for Fe and Cu using pyrite and Cu sulfide standards. The structures of Fe sulfides were identified using single-crystal SAED by tilting the crystals into zone-axis orientations.
8. There is uncertainty in the measured *d* spacings as a result of structural disorder in almost every part of this crystal.
9. A. R. Lennie *et al.*, *Am. Mineral.* **82**, 302 (1997).
10. R. De Médicis, *Science* **170**, 1191 (1970).
11. J. B. Murowchick and H. L. Barnes, *Am. Mineral.* **71**, 1243 (1986).
12. J. B. Murowchick, *Geol. Soc. Am. Progr. Abstr.* **21**, A120 (1989).
13. On the basis of the geometries of SAED patterns that were obtained from these crystals, they could be

- either [001], [111], [131], [313], and [232] projections of mackinawite or [001], [110], [112], [123], and [114] projections of cubic FeS, respectively (these patterns are not shown in the figures). The d_{200} spacings of cubic FeS and the crystallographically corresponding d_{110} spacings of mackinawite are 2.7 and 2.6 Å, respectively; the observed reflections have *d* values closer to cubic FeS than to mackinawite.
14. D. T. Rickard, *Stockholm Contrib. Geol.* **20**, 55 (1969).
15. M. A. A. Schoonen and H. L. Barnes, *Geochim. Cosmochim. Acta* **55**, 1505 (1991).
16. In the case of these small crystals embedded in bacterial cells, the analytical error is estimated to be about 0.1 formula unit Fe.
17. One month after sample collection, these crystals were still mackinawite or cubic FeS; they also contained a few atomic percent Cu, just like the disordered mackinawite-greigite magnetosomes. The cell was collected from Salt Pond, MA.
18. E. F. Bertaut, P. Burlet, J. Chappert, *Solid State Commun.* **3**, 335 (1965).
19. M. Wintenberger, B. Srour, C. Meyer, F. Hartmann-Boutron, Y. Gros, *J. Phys. (Paris)* **39**, 965 (1978).
20. D. A. Bazylinski *et al.*, *Appl. Environ. Microbiol.* **61**, 3232 (1995).

21. D. T. Rickard, *Stockholm Contrib. Geol.* **20**, 67 (1969).
22. R. A. Berner, *Am. J. Sci.* **265**, 773 (1967).
23. E. F. DeLong, R. B. Frankel, D. A. Bazylinski, *Science* **259**, 803 (1993).
24. R. B. Frankel, D. A. Bazylinski, M. S. Johnson, B. L. Taylor, *Biophys. J.* **73**, 994 (1997).
25. G. Wächtershäuser, *Syst. Appl. Microbiol.* **10**, 207 (1988); *Microbiol. Rev.* **53**, 452 (1988); R. J. P. Williams, *Nature* **343**, 213 (1990).
26. D. S. McKay *et al.*, *Science* **273**, 924 (1996).
27. R. E. Krupp, *Eur. J. Mineral.* **6**, 265 (1994).
28. B. J. Skinner, R. C. Erd, F. S. Grimaldi, *Am. Mineral.* **49**, 543 (1964).
29. W. Morse, F. J. Millero, J. C. Cornwell, D. Rickard, *Earth Sci. Rev.* **24**, 1 (1987).
30. We thank J. B. Murowchick, H. Hartman, and I. Dódonay for helpful discussions, B. Howes and D. R. Schlegler for help with sample collection, and W. H. Fowle for suggestions in the manipulation of magnetotactic microorganisms. Supported by grants from NSF and NASA. Electron microscopy was performed at the Center for High-Resolution Electron Microscopy at Arizona State University.

20 February 1998; accepted 19 March 1998

Clams As Recorders of Ocean Ridge Volcanism and Hydrothermal Vent Field Activity

Stanley R. Hart and Jerzy Blusztajn

The clam *Calyptogena magnifica* lives at abyssal depths in association with hydrothermal venting on midocean ridges. Analysis of strontium/calcium ratios in *C. magnifica* shells provides a temperature proxy with submonthly time resolution. A 21-year strontium/calcium record of two clams from 9°50'N on the East Pacific Rise captures the known 1991 and 1992 eruptive events, documents several additional events between 1992 and 1996, and demonstrates the absence of major hydrothermal episodes during the period 1974 to 1991. These clam archives can increase our understanding of the thermal and chemical history of midocean ridge hydrothermal and volcanic activity on decadal time scales.

Hydrothermal vent systems on midocean ridges influence the chemistry of the oceans in addition to acting as a semaphore for the underlying magmatic activity that drives them. The venting occurs as focused high-temperature flow ($>300^\circ\text{C}$ "hot smokers") and diffuse low temperature ($<50^\circ\text{C}$) flow. The hot smokers exhibit temporal variations in activity and chemistry over time scales that range from hourly (1) to millennial (2). The diffuse-flow venting, which accounts for 80 to 90% of the vent field fluid fluxes (3, 4), is poorly documented in temporal and spatial variability (5, 6). After the 1977 discovery of deep-sea vent systems, oxygen isotope compositions of shells of vent field clams were used to derive time series information on vent field activity (7, 8). The trace element chemistry of clams was investigated as a monitor of vent fluid chemistry (9, 10). Using ion microprobe techniques (11) we present Sr/Ca records

with submonthly temporal resolution for two *C. magnifica* shells from 10°N East Pacific Rise (EPR), covering the period 1974 to 1996 (12). The records show a gradual "warming" of activity in this area, culminating with the known 1991 and 1992 eruption events.

The clam *Calyptogena magnifica* lives in vent fields on midocean ridges, where it has access to warm water and nutrients (sulfide) associated with circulating hydrothermal fluids. It typically lives rooted into cracks and fissures within the basaltic flows where warm (up to 20°C) diffuse venting occurs (13). *Calyptogena magnifica* appears to be only marginally mobile (14, 15) and commonly dies if crowded out of a fissure or if the local venting shuts down (14, 16). The clams have a fairly well-understood von Bertalanffy-type growth modality (8, 17–19). Initial growth rates of centimeters per year slow to <1 mm/year as the clam ages. Life spans of nearly 50 years have been documented (20, 21); mortality results either from extreme excursions of vent activ-

Woods Hole Oceanographic Institution, Woods Hole, MA 02543, USA.

ity or by the continuous carbonate dissolution of the unprotected shell of *C. magnifica*. Estimates of survival times of 15 to 25 years for shells of dead clams (7, 19) have been extended to several centuries, provided the shells remain out of contact with warm vent fluids (22). Time series records of several decades should be possible with live clams, and multicentury records are a possibility in optimal situations.

Trace elements in biogenic carbonates can be used as temperature proxies. The content of a carbonate trace element, M , is related to that in the coexisting water through an exchange coefficient, K_D :

$$K_D = \left(\frac{M}{Ca} \right)^{\text{carbonate}} / \left(\frac{M}{Ca} \right)^{\text{water}}$$

where K_D is typically a function of temperature as well as of biological and growth rate controls (usually lumped together as "vital effects"). No calibrations of K_D have been done for *Calypptogena*; we have calibrated Sr/Ca in an *Arctica islandica* (23) and use this as a *Calypptogena* analog, in view of the structural, morphologic (24, 25), and chemical similarities (26) of these two bivalve genera.

Sample 2498 was collected live on 7 March 1992 from within the axial summit trough (AST) and sample 3068F was collected live on 19 April 1996 just east of the AST (Fig. 1). The two localities are 50 m apart and about 300 m from the nearest hot smoker (Q vent). The AST on this segment of the EPR experienced an eruption in March/April 1991 (27) and a second eruption in January/February 1992 (28).

The Sr/Ca time series for clam 2498

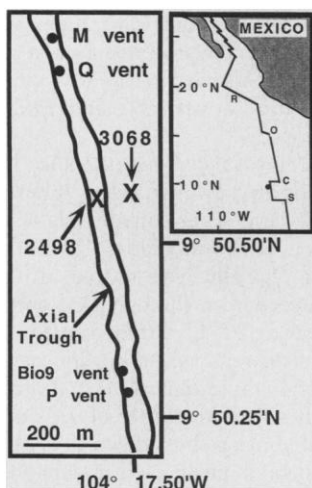


Fig. 1. Location map of the EPR at 9°50'N showing the collection sites of *C. magnifica* specimens 2498 and 3068F in relation to nearby hot smoker vents and the walls of the AST (39). R, O, C, and S, Rivera, Orozco, Clipperton, and Siguieros fracture zones.

(Fig. 2A), with an estimated age of 23 years (29), shows a long, relatively cool (<10°C) and featureless early life period (around 1974 to 1984) followed by a trend of increasing temperature, with marked variability. The record culminates with a sharp spike (at ~72 mm) followed by the beginning of a second spike. Because this clam was collected several months after the 1992 eruption, we interpret the final Sr/Ca increase to reflect the thermal anomaly associated with this eruption. The sharp spike at 72 mm is interpreted to mark the March/April 1991 eruption.

The Sr/Ca record for the second clam (Fig. 2B) is strikingly similar to that of the first, starting with the stepwise jump in Sr/Ca at 40 mm. This step is followed by a

long undulating but gradual decline, followed by a rapidly increasing Sr/Ca, with significant short-term variability, starting at ~55 mm in clam 2498 and at ~50 mm in clam 3068F. The peaks in clam 2498 inferred to reflect the 1991 and 1992 eruptions are also observed in clam 3068F at 54.4 and 56.3 mm. Because clam 3068F was collected 4 years after clam 2498, the additional Sr/Ca record during this time period shows one large and two smaller Sr/Ca peaks (designated A, B, and C, Fig. 2B).

Much of the Sr/Ca range exhibited by the last few years of the *Calypptogena* record is higher than the range calibrated in the *Arctica* (23). There is also a small change in Sr/Ca of vent fluid correlated with temperature (30). Extrapolation to the high Sr/Ca

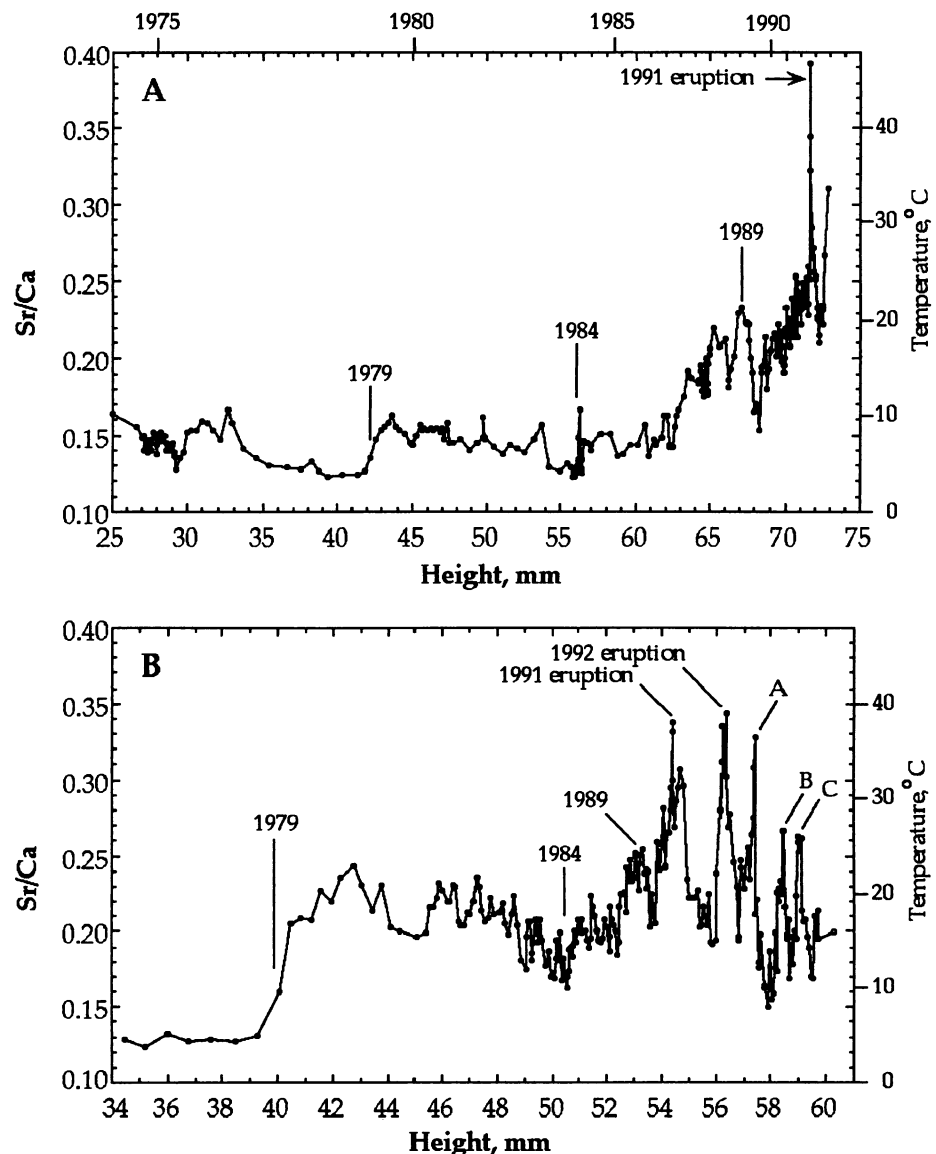


Fig. 2. Sr/Ca ratios (as $^{88}\text{Sr}/^{42}\text{Ca}$ ion ratios) versus height along an umbo (=0 mm) to ventral edge cross section of the left valves of *C. magnifica* specimens 2498 (A) and 3068F (B). The oldest points are close to the outcrop of the pallial myostracum (9). See (23) for temperature calibration. Specimens were provided by D. Fornari and C. Cavanaugh.

of the 1991 peak would infer temperatures in excess of 45°C. This is higher than any direct evidence regarding the temperature limits of *C. magnifica* (13, 14), although temperatures up to 55°C have been recorded for diffuse flow activity associated with the 1991 eruption (31). It is known that *Calyptogena* frequently live in flow environments where temperature gradients of 10° to 20°C are present between anterior and posterior ends (14). With the adopted temperature calibration, it appears that these clams spent most of their early lives at temperatures close to ambient (1.8°C at this locality); the segments at 35 to 40 mm (Fig. 2A) and around 34 to 39 mm (Fig. 2B) are equivalent to temperatures of 4° to 5°C.

Accepting the identification of the 1991 and 1992 eruption peaks and the known harvesting dates for both clams, we can calculate growth rates for various time intervals. For the interval between the 1991 and 1992 eruptions, clam 2498 grew 1.3 mm/year and clam 3068F grew 2.1 mm/year. For the interval between the 1992 eruption and the collection date of clam 3068F, the growth rate was 0.9 mm/year. Accepting the step increase in both clams at 40 to 42 mm as isochronous, clam 2498 grew twice as fast as clam 3068F between this time and the 1991 peak. Probably no single growth curve is applicable to both clams, because *C. magnifica* relies on sulfide in the vent fluids for nourishment (via the chemosynthetic endosymbionts hosted by the clam). The thermal variability recorded by the Sr/Ca proxy is necessarily accompanied by variability in the nutrient supply, assuming that temperature and sulfide behave conser-

vatively during mixing of seawater and hot smoker fluid.

Although *C. magnifica* require warm sulfide-laden water for growth, there may be a limit where further increases in temperature adversely affect growth rates, despite the still increasing sulfide supply (sulfide may reach a level where the clams become unable to detoxify blood sulfide levels by complexation) (32, 33). This may be the explanation for the slower growth rate of clam 3068F between the "step" and the 1991 eruption peak; during this interval clam 3068F is recording temperatures in the 10° to 25°C range, and clam 2498 is residing in a cooler (<10°C) environment. We tentatively place the optimal temperature and nutrient range for *C. magnifica* somewhere around 10° to 15°C.

The higher average temperatures recorded by clam 3068F from 1979 to 1991 are also reflected in its greater extent of dissolution. The surface "outcrop" of the pallial myostracum (8) (where the older outer shell layer is completely dissolved) is much closer to the ventral edge in clam 3068F than in clam 2498 (53% versus 28% of the height). This may reflect both the greater undersaturation of carbonates in warm acidic vent fluids and the kinetic effect of temperature on dissolution rates (a temperature increase from 5° to 20°C increases calcite dissolution rates by a factor of about 2.7) (34).

Assigning absolute time scales to the growth records of these clams will be difficult until precise radiometric dating is available (20, 21). Based on the height of clam 2498, the two bounding growth mod-

els of Lutz *et al.* (19) suggest ages of 10.7 and 23.0 years. The growth model of (8) gives an intermediate age (15.5 years). When the measured growth rate between the 1991 and 1992 eruptions is used ages of 22 and 28.5 years are calculated for the bounding growth models of (19). If we assume a single growth model throughout its life, the height and 1991 to 1992 growth rate of clam 2498 can be combined to specify a new growth model with a unique solution for age at capture of 30.9 years (35). We consider this age a maximum, as the 1991 to 1992 growth rate is likely to be lower than normal rates because of the higher temperatures during this period.

Recognizing the nonuniqueness of these age estimates, we will adopt the 21°N growth model (29) for clam 2498 as a first approximation. The age at capture is then 23.0 years, the birth date is 1969.2, the date of the step increase at 42.0 mm height is 1979.0, and the beginning of the period of increasing temperatures (~56 mm) is 1984.0.

For clam 3068F, the step increase at 40 mm becomes 1979.0 (by correlation with clam 2498). Using the 21°N growth model for the pre-1979 record, the birth date for this clam is 1969.8 (~0.6 years younger than clam 2498). The average growth rate from birth to the 1979 step is 4.3 mm/year, from 1979 to the 1991 eruption it is 1.2 mm/year, between the 1991 and 1992 eruptions it is 2.1 mm/year, and from the 1992 eruption to collection it is 0.9 mm/year. Approximate age assignments of the three post-1992 temperature spikes (A, B, and C, Fig. 2B) are 1993.2, 1994.3, and 1994.8. The prominent valley between peaks A and B, with temperatures of only 8°C, dates to about 1993.7.

Temperature recorders in the region 9°50'N recorded (Fig. 3) an abrupt step increase from 4° to 23°C at Bio9 vent on 5 July 1994 and farther south a diffuse flow temperature peak of 17°C was recorded in August 1994 (5). This timing correlates with either peak B or C. Another temperature increase (to at least 24°C) was recorded in October 1995 (Fig. 3); this does not appear to correlate with the Sr/Ca record, although this time period was only a few months before collection of clam 3068F. Peak A (~1993.2) cannot be directly corroborated as there were no temperature recorder deployments or Alvin dives during this time period. Based on the size of peak A relative to the 1991 and 1992 eruption-related peaks, we postulate that a third magmatic/tectonic event occurred in early 1993 that affected the hydrothermal system but has not been recognized in the geomorphic or observational record. The low-temperature valley be-

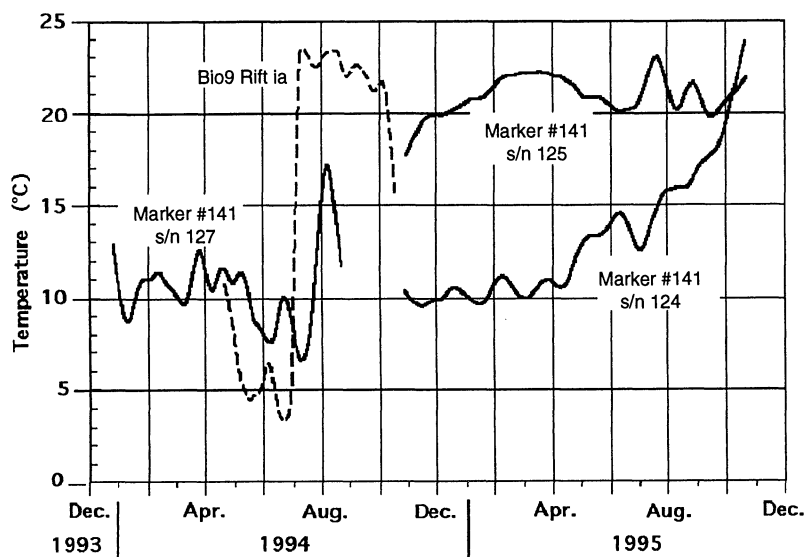


Fig. 3. Temperature records from the Bio9 (Fig. 1) and Biomarker 141 areas of the EPR. Biomarker 141 is within the AST about 830 m south of Bio9. Temperatures were derived from miniloggers (6) deployed on the basaltic pavement in areas of diffuse flow venting. Recorders s/n 125 and s/n 124 were 10 cm apart. Data from Fornari *et al.* (40) [see also Shank *et al.* (5)].

tween peaks A and B in Fig. 2B is consistent with Alvin observations in December 1993 of waning hydrothermal activity along much of this ridge crest area (31).

REFERENCES AND NOTES

1. K. L. Von Damm, *Geophys. Monogr. Am. Geophys. Union* **91**, 222 (1995).
2. C. Lalou *et al.*, *J. Geophys. Res.* **98**, 9705 (1993).
3. D. Kadko, *Rev. Geophys.* **34**, 349 (1996).
4. H. Elderfield and A. Schultz, *Annu. Rev. Earth Planet. Sci.* **24**, 191 (1996).
5. T. M. Shank *et al.*, *Eos* **76**, F701 (1995).
6. D. Fornari, F. Voegeli, M. Olsson, *RIDGE Events* **7**, 13 (1996).
7. J. S. Killingley, W. H. Berger, K. C. MacDonald, W. A. Newman, *Nature* **287**, 218 (1980).
8. M. Roux, M. Rio, E. Fatton, *Bull. Biol. Soc. Wash.* **6**, 211 (1985).
9. G. Roesijadi and E. A. Crecelius, *Mar. Biol.* **83**, 155 (1984).
10. C. Chassard-Bouchaud, A. Fiala-Medioni, P. Galle, *C. R. Acad. Sci.* **302**, 117 (1986).
11. The Cameca 3f ion probe at Woods Hole Oceanographic Institution was used for all Sr/Ca analyses and follows the technique of (36). Spot size was 30 to 40 μm . Drift and intercalibration utilized a natural calcite standard mounted with each specimen. The accuracy of a single spot analysis is better than $\pm 1.6\%$ (2 σ). The ion ratio conversion is Sr/Ca mole ratio = $0.00771^{86}\text{Sr}/^{42}\text{Ca}$ ion ratio.
12. S. R. Hart and J. Blusztajn, in *Seventh Annual V. M. Goldschmidt Conference, LPI Contribution No. 921* (Lunar and Planetary Institute, Houston, 1997), p. 89.
13. C. R. Fisher *et al.*, *Deep Sea Res.* **35**, 1811 (1988).
14. R. R. Hessler, W. M. Smithey, C. H. Keller, *Bull. Biol. Soc. Wash.* **6**, 411 (1985).
15. V. Tunnicliffe, *Oceanogr. Mar. Biol. Annu. Rev.* **29**, 319 (1991).
16. R. A. Lutz and M. J. Kennish, *Rev. Geophys.* **31**, 211 (1993).
17. M. Rio and M. Roux, *C. R. Acad. Sci.* **299**, 167 (1984).
18. R. A. Lutz, L. W. Fritz, D. C. Rhoads, *Biol. Soc. Wash. Bull.* **6**, 199 (1985).
19. R. A. Lutz, L. W. Fritz, R. M. Cerrato, *Deep Sea Res.* **35**, 1793 (1988).
20. K. K. Turekian and J. K. Cochran, *Science* **214**, 909 (1981).
21. ———, J. T. Bennett, *Nature* **303**, 55 (1983).
22. M. J. Kennish, R. A. Lutz, A. S. Pooley, *RIDGE Events* **8**, 6 (1997).
23. A Sr/Ca record for 1956 to 1963 was determined for a 38-year-old *Arctica islandica* collected in 1991 at 60-m depth near the Nantucket Shoals Lightship. See (37) for a $\delta^{18}\text{O}$ time series. Weekly bottom water temperature records for this site were matched with Sr/Ca amplitudes to give a temperature calibration of $T^\circ\text{C} = 20,752 [\text{Sr}/\text{Ca} (\text{mol}/\text{mol})] - 16.0$. Slope and intercept errors of the regression line are $\pm 9.6\%$ and $\pm 3.0^\circ\text{C}$ (1 σ).
24. J.-J. Oberling and K. J. Boss, *Rev. Suisse Zool.* **77**, 81 (1979).
25. K. J. Boss and R. D. Turner, *Malacologia* **20**, 161, (1980).
26. B. F. Mg, Sr, and Ba contents in a 2-year interval in the *Arctica* specimen were similar (5 to 30%) to the 1975 to 1979 segment of *Calyptogenia* 2498.
27. R. M. Haymon *et al.*, *Earth Planet. Sci. Lett.* **119**, 85 (1993).
28. K. H. Rubin, J. D. Macdougall, M. R. Perfit, *Nature* **368**, 841 (1994).
29. The ^{21}N EPR age model (19) is as follows: age = $-20.921 \ln[1.0222 - 0.00946 \times \text{height} (\text{mm})]$.
30. The fluid Sr/Ca ratio is not independent of temperature because the Sr/Ca of the diffuse fluid end member is $\sim 34\%$ that of ambient seawater (38). At 20°C , this effect is -0.38% per $^\circ\text{C}$; the temperature dependence is $+2.3\%$ per $^\circ\text{C}$. Our temperatures may be underestimated by up to 10°C at 50°C .
31. T. M. Shank *et al.*, *Deep Sea Res.*, in press.
32. J. J. Childress, C. R. Fisher, J. A. Favuzzi, N. K. Sanders, *Physiol. Zool.* **64**, 1444 (1991).
33. M. J. Kennish and R. A. Lutz, *Rev. Aquat. Sci.* **6**, 29 (1992).
34. Z. Liu and W. Dreybrodt, *Geochim. Cosmochim. Acta* **61**, 2879 (1997).
35. The 1991 to 1992 growth rate occurs at the same age as the observed 1991.5 height when height = $107 - 104.65 \exp(-0.0363t)$.
36. S. R. Hart and A. L. Cohen, *Geochim. Cosmochim. Acta* **60**, 3075 (1996).
37. C. R. Weidman, G. A. Jones, K. C. Lohmann, *J. Geophys. Res.* **99**, 18305 (1994).
38. R. H. James and H. Elderfield, *Geology* **24**, 1147 (1996).
39. D. J. Fornari, R. M. Haymon, M. R. Perfit, T. K. Gregg, M. H. Edwards, *J. Geophys. Res.*, in press.
40. D. Fornari, T. Shank, R. Lutz, unpublished data.
41. We are indebted to D. Fornari for his many unselfish contributions to this project. The in situ temperature data were generously provided by D. Fornari, R. Lutz, and T. Shank. Discussions, comments, and reviews by D. Fornari, G. Ravizza, L. Mullineaux, and K. Turekian were most helpful. This work was carried out with the support of the C. O. Iselin Chair.

20 October 1997; accepted 13 March 1998

Pressure-Induced Amorphization and Negative Thermal Expansion in ZrW_2O_8

C. A. Perotoni and J. A. H. da Jornada*

It has recently been shown that zirconium tungstate (ZrW_2O_8) exhibits isotropic negative thermal expansion over its entire temperature range of stability. This rather unusual behavior makes this compound particularly suitable for testing model predictions of a connection between negative thermal expansion and pressure-induced amorphization. High-pressure x-ray diffraction and Raman scattering experiments showed that ZrW_2O_8 becomes progressively amorphous from 1.5 to 3.5 gigapascals. The amorphous phase was retained after pressure release, but the original crystalline phase returned after annealing at 923 kelvin. The results indicate a general trend between negative thermal expansion and pressure-induced amorphization in highly flexible framework structures.

Pressure-induced amorphization is a phenomenon of widespread occurrence among framework structures, and many recent theoretical and experimental investigations have been devoted to extending our understanding of the underlying mechanisms (1, 2). Disordered phases can be generated upon compression and decompression and even during indentation hardness tests (2, 3). Several mechanisms have been proposed to explain the process of pressure-induced amorphization in solids, including melting effects and kinetically frustrated phase transitions to another crystalline state, as well as the failure of some criterion of lattice stability (1, 2). Some compounds, including ice and silicon, that under special conditions transform to an amorphous phase under pressure also exhibit negative thermal expansion, at least within a limited range of temperature. Recent computer simulations pointed out the possibility of a common origin between pressure-induced amorphization and negative thermal expansion in tetrahedrally bonded networks (4).

The remarkable behavior of ZrW_2O_8 , a cubic compound that contracts on heating, has been known for the past 30 years (5). Recent measurements have shown that

ZrW_2O_8 exhibits isotropic negative thermal expansion over its entire range of stability, from 0.3 to 1050 K (6, 7). This property makes zirconium tungstate an ideal candidate for investigating the relation between contraction on heating and pressure-induced amorphization in framework structures.

The crystal structure of ZrW_2O_8 at ambient conditions can be described as a framework of corner-sharing ZrO_6 octahedra and WO_4 tetrahedra. In each WO_4 tetrahedron, one of the oxygen atoms is bonded to only one tungsten atom, resulting in a structure with great flexibility. This compound undergoes a structural phase transition at about 430 K, from space group $P2_13$ to $Pa\bar{3}$, which hardly affects the negative thermal expansion coefficient (6, 7). Recently, Evans and co-workers showed that upon compression above 0.2 GPa, cubic ZrW_2O_8 transforms to a quenched orthorhombic phase (space group $P2_12_12_1$), which also exhibits negative thermal expansion, although reduced by one order of magnitude (8).

The great flexibility of the ZrW_2O_8 framework seems to be the key to its unusual properties (9). Because of this high flexibility, some low-energy vibrational modes can propagate through the structure without distortion of the ZrO_6 and WO_4 building blocks. These vibrational modes, called rigid unit modes (RUMs), have been successfully applied to the study of properties

Universidade Federal do Rio Grande do Sul, Instituto de Física, 91501-970 Porto Alegre-RS, Brazil.

*To whom correspondence should be addressed. E-mail: jornada@if.ufrgs.br